Life Sciences 310 (2022) 121046

Contents lists available at ScienceDirect

Life Sciences

journal homepage: www.elsevier.com/locate/lifescie

Matrix metalloproteinase 2 is a target of the RAN-GTP pathway and mediates migration, invasion and metastasis in human breast cancer

Mohamed El-Tanani [a,c,*], Angela Platt-Higgins [e], Yin-Fai Lee [b,h], Arwa Omar Al Khatib [a], Yusuf Haggag [d], Mark Sutherland [g], Shu-Dong Zhang [c,f], Alaa A.A. Aljabali [j], Vijay Mishra [k], Ángel Serrano-Aroca [l], Murtaza M. Tambuwala [i,**], Philip S. Rudland [e]

[a] Pharmacological and Diagnostic Research Centre, Al-Ahliyya Amman University, Faculty of Pharmacy, Amman, Jordan
[b] Neuroscience, Psychology & Behaviour, College of Life Sciences, University of Leicester, Leicester LE1 9HN, UK
[c] Institute of Cancer Therapeutics, Faculty of Life Sciences, University of Bradford, Bradford, UK
[d] Department of Pharmaceutical Technology, Faculty of Pharmacy, Tanta University, Tanta, Egypt
[e] Institute of Systems, Molecular and Integrative Biology, University of Liverpool, Liverpool, UK
[f] Northern Ireland Centre for Stratified Medicine, Biomedical Sciences, University of Ulster, UK
[g] School of Chemistry and Biomedical Sciences, University of Bradford, Bradford, UK
[h] School of Life Sciences, Faculty of Science and Engineering, Anglia Ruskin University, Cambridge CB1 1PT, UK
[i] School of Pharmacy and Pharmaceutical Science, Ulster University, Coleraine BT52 1SA, UK
[j] Department of Pharmaceutics and Pharmaceutical Technology, Yarmouk University, Irbid, Jordan
[k] School of Pharmaceutical Sciences, Lovely Professional University, Phagwara 144411, Punjab, India
[l] Biomaterials and Bioengineering Lab, Centro de Investigación Traslacional San Alberto Magno, 16 Universidad Católica de Valencia San Vicente Mártir, c/Guillem de Castro 94, 46001, Valencia, Spain

ARTICLE INFO

Keywords:
RAN-GTP
MMP2
ATF3
CXCR3
Cell migration
Breast cancer
Patient survival
cMet
cMyc and Ki67

ABSTRACT

RAS-related nuclear protein(RAN) is a nuclear shuttle and normally regulates events in the cell cycle. When overexpressed in cultured cells, it causes increases in cell migration/invasion in vitro and its overexpression is associated with early breast cancer patient deaths in vivo. However, the underlying mechanism is unknown. The effect of RAN overexpression on potential targets MMP2, ATF3, CXCR3 was investigated by Real-Time PCR/Western blots in the triple receptor negative breast cancer(TRNBC) cell line MDA-MB231 and consequent biological effects were measured by cell adhesion, cell migration and cell invasion assays. Results showed that knockdown of RAN lead to a reduction of MMP2 and its potential regulators ATF3 and CXCR3. Moreover, knockdown of ATF3 or CXCR3 downregulated MMP2 without affecting RAN, indicating that RAN regulates MMP2 through ATF3 and CXCR3. Knockdown of RAN and MMP2 reduced cell adhesion, cell migration and cell growth in agar, whilst overexpression of MMP2 reversed the knockdown of RAN. Furthermore, immunohistochemical staining for RAN and MMP2 are positively associated with each other in the same tumour and separately with patient survival times in breast cancer specimens, suggesting that a high level of RAN may be a prerequisite for MMP2 overexpression and metastasis. Moreover, positive immunohistochemical staining for both RAN and MMP-2 reduces further patient survival times over that for either protein separately. Our results suggest that MMP2 expression can stratify progression of breast cancers with a high and low incidence of RAN, both RAN and MMP2 in combination can be used for a more accurate patient prognosis.

Simple summary: Ran is an important regulator of normal cell growth and behaviour. We have established in cell line models of breast cancer (BC) a molecular pathway between RAN and its protein-degrading effector MMP-2 and properties related to metastasis in culture. Using immunohistochemistry (IHC) staining of primary BCs, we have shown that RAN and MMP-2 are on their own significantly associated with patient demise from metastatic BC. Moreover, when staining for MMP-2 is added to that for RAN in the primary tumours, there is a significant

Abbreviations: MMP2, Matrix metalloproteinase 2; BC, breast cancer; ATF3, activating transcription factor 3; CXCR3, C-X-C motif chemokine receptor 3.

* Correspondence to: M. El-Tanani, Pharmacological and Diagnostic Research Centre, Al-Ahliyya Amman University, Faculty of Pharmacy, Amman, Jordan.
** Corresponding author.
E-mail addresses: m.el-tanani@bradford.ac.uk (M. El-Tanani), m.tambuwala@ulster.ac.uk (M.M. Tambuwala).

https://doi.org/10.1016/j.lfs.2022.121046
Received 4 July 2022; Received in revised form 29 September 2022; Accepted 2 October 2022
Available online 6 October 2022

decrease in patient survival time over that for either protein alone. Thus a combination of staining for RAN and MMP2 is an excellent marker for poor prognosis in breast cancer.

1. Introduction

Worldwide, there are an estimated 1 million cases and 0.5 million deaths from breast cancer (BC) annually [1], but the underlying mechanisms that cause metastasis and ultimately death are largely unknown. One molecule RAS-related nuclear protein, RAN is overexpressed in the primary tumours of breast cancer, and its overexpression is associated with a decrease in survival times of the corresponding patients [2,3], presumably resulting from enhanced metastasis of the primary tumours [2]. RAN itself is a small GTPase [4] which is highly conserved in eukaryotes and is essential for cell viability [4]. It is involved in various cellular processes including nucleocytoplasmic transport, mitotic spindle organization and nuclear envelope formation [5]. RAN regulates formation and organization of the microtubule network independently of its role in the nuclear-cytosol exchange of macromolecules [6] and it also appears to be a key signalling molecule regulating microtubule polymerization during cell adhesion and cell migration [6].

Recently, we have shown that when an expression vector for RAN is transfected into benign, non-invasive rat mammary (Rama 37) cells, it has the ability to transform their phenotype, producing increased cell migration and invasion in vitro and the induction of metastasis in syngeneic rats in vivo [7]. Silencing RAN using small interfering RNAs reversed the induction of this metastatic phenotype [7,8]. However, how RAN induces these changes is unknown. Here we identify a matrix metalloproteinase (MMP), MMP2 [9], and its upstream regulators, activating transcription factor 3 (ATF3) [10–16] and C-X-C motif chemokine receptor 3 (CXCR3) [17,18] that are targets for the RAN-induced increases in metastasis-related properties in vitro and show a signification association between immunohistochemical staining for RAN, MMP2 in the primary tumours and survival time of breast cancer patients in vivo. We also show that staining for MMP2 acts synergistically with that for RAN in their association with survival times and use staining for MMP2 and RAN in combination to obtain a more accurate prognosis for the patient.

2. Materials and methods

2.1. Culture conditions

The TRNBC MDA-MB231, estrogen receptor-positive MCF-7,T47D breast cancer cell lines and viral packaging cell line 293T (HEK) were obtained from the American Type Culture Collection (ATCC), Manassas, VA, USA and maintained in Dulbecco's modified Eagle's medium (DMEM) containing 10 % (v/v) fetal bovine serum (FBS), 2 mM L-glutamine, and 1 % (v/v) penicillin and streptomycin in an atmosphere of 90 % (v/v) air, 10 % (v/v) CO_2. Cells were cultured in normal medium [2] until 24 h post-infection and used within 20 passages on receipt [7]. Cells were harvested at 72 h post-infection for mRNA extraction and protein blotting, unless otherwise specified, as previously described [2,3,19] Expression of mRNA, Western blotting, adhesion to fibronectin, colony growth in agar and invasion assays were analysed after 48 h post infection, as previously described [2]. The Institute of Cancer Therapeutics, University of Bradford analysed the cell lines for potential mycoplasma contamination and authentication.

2.2. Transfection and infection

Infections or transductions were performed using GeneJuice® (Promega, Southampton, UK). Viral particles were harvested 48 h post-transfection and were applied to the target cells with 6 μg/ml polyprene supplement for 4 h and then refreshed. The same amount and same batch of viral particles were used for any comparisons made in the present study. Cell lines were designated shRAN for cell lines transduced with short hairpin (sh) RNA for RAN, shMMP2 for cell lines transduced with short hairpin RNA to MMP2 and shScr for cell lines transduced with scrambled, noncoded shRNA (Sigma-Aldrich, Dorset, UK), as previously described [19].

2.3. Generation of cell lines

pLKO.1-shRAN1, -2, and -3 (clone IDs: NM 006325.2s1cl, NM 006325.2-198s1c1, and NM 006325.2-484s1c1, respectively) were purchased from Sigma-Aldridge, and pBABE-puro was purchased from Addgene (Cambridge, MA). Scr (#1864). pLKO.1-shScramble stable transfection was used to generate MDA-MB231 pBabe-vector and MDA-MB231 pBabe-shMMP2 cells by selecting cells with the appropriate concentrations of antibiotics. Retroviral infection of pBabe-vector and pBabe-shMMP2 plasmids yielded MDA-MB231-vector and MDA-MB231-shMMP2 cells, respectively. MDA-MB231-shScr and MDA-MB231-shRAN1, -2, and -3 cells were generated by lentiviral infection of pLKO.1-shScr and pLKO.1-shRAN1, -2, and -3, respectively, as previously described [2,3]. The stable cells were used only when they were within 5 passages after establishment.

2.4. Real-time polymerase chain (RT-PCR)

RNA was extracted using Trizol (Invitrogen, Paisley, UK) and reverse transcription was performed using SuperScript™ III first strand synthesis system (Invitrogen) according to the manufacturer's instructions. Total RNA was isolated using the TRIZol reagent (Invitrogen) and reverse transcription was performed using SuperScript™ III first strand synthesis system (Invitrogen), according to the manufacturer's instructions. The concentration of purified RNA was determined in a Agilent 2100 bioanalyzer using RNA 6000 NanoChips (Agilent, Waldbronn, Germany). qRT-PCR was performed using the QuantiTect SYBR Green RT-PCR kit (Qiagen, Hilden, Germany) on a DNA Engine Opticon (Bio-Rad, Loanhead, UK). All reactions were performed with 500 ng of total RNA in a volume of 25 μl. The expression level of each gene was quantified using the $2^{-\Delta\Delta Ct}$ method [20]. Real-time PCR was performed according to the manufacturer's instructions (Applied Biosystem, Foster City, CA) using a Taqman® assay for RAN (Hs01044225_g1), for MMP-2 (Hs01548727_m1), for ATF3 (Hs00231069_m1) and for CXCR3 (Hs01847760_s1) from Applied Biosystems. Data are the mean of three independent experiments ± SD. All results were normalized using a housekeeping gene, β-actin as previously described [2,3,19,21].

2.5. Western blot

Western blotting was performed as previously described [2,3]. Briefly, cells were lysed in RIPA buffer containing protease inhibitors. The samples were separated by 8 % (w/v) SDS-PAGE and transferred onto a nitrocellulose membrane (Millipore, Watford, UK). The membranes were blocked with 5 % (v/v) nonfat dried milk in PBS and subsequently incubated with primary antibodies as follows: anti-RAN (1:1000) from Biosciences, anti-CXCR3 (1:1000) from Sigma, anti-ATF3 (1:1000) and anti-MMP2 (1:1000) from Merck, overnight at 4 °C (Supplementary Table S1) Bound antibodies were detected by horseradish peroxidases-conjugated secondary antibodies at 1:10,000 incubated at RT for 1 h with enhanced chemiluminescence (Amersham Pharmacia Biotech, Chalfont, UK) for detection. Densitometry on scanned immunoblot images was performed using the ImageJ software. Data are the mean of three independent experiments ± SD. All results were

normalized using a housekeeping gene, β-actin and quantified using densitometry readings [2,3].

2.6. Cell adhesion assay

For the cell the adhesion assay, 40,000 cells/well in normal medium were seeded in a 96-well plate coated with fibronectin and allowed to settle for 30 min. Suspended cells were removed by washing 4 times with PBS. Adhered cells were fixed and stained with crystal violet. The excess dye was washed out and the retained dye was extracted. The absorbance at 595 nm was measured in a microplate reader. Data are the mean of three independent experiments ± SD, as previously described [2].

2.7. Boyden chamber migration and invasion assays

Migration and invasion assays were performed as previously described [2]. Briefly, 5000 and 50,000 cells in serum-free conditions were seeded into the upper Boyden chamber (Millipore) on top of the membrane without or with a Matrigel coating for migration and invasion assays, respectively. The cells were allowed to migrate/invade towards the underside for 24 h with 10 ng/ml hepatocyte growth factor (HGF) as a chemoattractant. Cells on the underside of the membrane were fixed and stained with crystal violet solution. Data are the mean of three independent experiments ± SD, as previously described [2].

2.8. Colony formation assay

Soft agar assay was performed as previously described [3]. 5000 suspension cells in normal medium containing 0.35 % (w/v) low-melting-point agarose were overlaid onto a solidified normal medium containing 0.7 % (w/v) low-melting-point agarose. Cells were incubated at 37 °C with 95 % (v/v) air, 5 % (v/v) carbon dioxide for 2 to 3 weeks. Colonies were visualized by staining with crystal violet. The colonies were viewed directly in a microscope at an appropriate magnification and a range of 10 to 100 colonies were counted per field, 10 fields per plate and 3 plates per experiment. Data are the mean of three independent experiments ± SD [2,3,21–25].

2.9. Patients and specimens

A retrospective study was undertaken using samples of 181 primary tumours from breast cancer patients as described previously [26]. Briefly, patients received no adjuvant therapy including hormonal therapy and only patients with operable breast cancer (T1-4, N0-1) were included. Patient follow-up times ranged from 14.5 to 19.4 years (mean 16.4 ± 0.1 years) with a mean ± SE survival time of 9.0 ± 0.5 years. Details of patients and their tumours are shown in Supplementary Table S2. Ethical approval was obtained from NRES Committee North West REC, Ref 12/NW/0778, Protocol no. UoL000889, IRAS no 107845. Samples were preserved in neutral buffered formalin and embedded in paraffin wax as described previously [26].

2.10. Immunohistochemical (IHC) staining

Histological sections cut at 4 μm were mounted on slides, treated with 0.05 % (v/v) H_2O_2 in methanol to inhibit endogenous peroxidase [26] and incubated with the relevant primary and then secondary horseradish peroxidase labelled antibodies/polymers in kits (DAB) (Dako Ltd., Ely, UK), as described previously [2]. Positive staining corresponded to an oxidised brown precipitate of diaminobenzidine (DAB). Slides were finally mounted in Glycergel mounting medium (Dako). Blocked antibodies prepared by mixing 1 mg/ml of the relevant blocking peptide/protein abolished this staining. Appropriate non-immune serum also yielded no staining. Western blots of breast cancer cell lines verified the specificity of all antibodies used by yielding the appropriately-sized molecular weight bands on SDS – polyacrylamide gels. IHC staining details for RAN [2,3] and MMP2 [27] and their validation have been extensively reported in another context in our previous publications [2,3,27].

2.11. IHC scoring analysis

IHC-stained sections were analysed and scored by two independent observers using light microscopy according to the percentage of stained carcinoma cells from 2 well separated sections of each specimen, 10 fields per section at 200× magnification and a minimum of 200 cells per field, as described previously [3,19,27]. Staining for all proteins had already been separated into two categorical groups, a negative and positive group with a cut-off of either 1 % or 5 % of carcinoma cells staining, according to which cut-off yielded the more significant difference and greater relative risks: 1 % cut-offs for RAN, cMyc, Ki67, CK5/6 and 5 % cut-offs for cMet, MMP2, ERα, c-erbB-2, PgR [2,3,26]. The association of staining for each protein separately in this set of patients was calculated from life tables constructed from survival data using Kaplan Meier plots and analysed by Wilcoxon (Gehan) statistics [2,3,26]. Patients who died from causes other than cancer were censored. Unadjusted relative risk (RR) for survival with 95 % confidence interval (95 % CI) was calculated using Cox's univariate analysis [2,3,26]. Association of IHC staining for RAN or MMP2 with other tumour variables was assessed by cross-tabulations using Fisher's Exact test (2-sided) using either 1 % or 5 % cut-offs. For multiple comparisons the resultant *P* values were corrected by the Holm-Bonferroni formulae of $1\text{-}(1\text{-}P)^n$, where n is the number of tumour variables. Binary Logistic Regression was used for calculation of the relative independent association (RA) of staining for one protein with the remaining proteins in the group. To determine if the association of patient survival with RAN, MMP2 etc. was significant within a group of proteins, Cox's multivariate analyses were performed on 181 patients, incomplete data arose mainly from lack of sampling [2,3,26]. Data analysis was performed using Excel (Microsoft, Redmond, WA), and SPSS version 22 (SPSS, Chicago, IL). The sensitivity and specificity, positive predictive response (PPR) and negative predictive response (NPP) were calculated using 1 % and 5 % staining cut-offs for RAN and MMP-2, respectively.

2.12. Statistical analysis

Statistical analysis on cell cultures was performed using SPSS 19.0 software (IBM, Armonk, NY). Differences between groups in in vitro experiments were tested by Student's *t*-test (two groups) and by analysis of variance (ANOVA) with post hoc Games–Howell adaptation for groups of 3 or more. Differences in immunohistochemical positivity of tumours between samples in the human specimens were analysed by Chi [2], Fisher's Exact test, or Mann–Whitney *U* tests, where applicable. The association between positive staining and patient survival was recorded by Kaplan–Meier plots and compared by Wilcoxon–Gehan tests. A *P* value of <0.05 was considered to be a statistically significant difference. All statistical tests were two-sided. $P < 0.05$, $^{**}P < 0.01$, $^{***}P < 0.001$ compared with control.

3. Results

3.1. Knockdown of RAN results in the downregulation of MMP2 in cancer cell lines

Previously, we had shown that knockdown of RAN using potent shRNAs results in apoptosis and changes in cell properties including cell adhesion, migration and invasion in the TRNBC cell line MDA-MB231 [2,3]. Hence the same 3 shRNAs to RAN: shRAN1, shRAN2 and shRAN3 were separately used to infect MDA-MB231 cells to produce the stable transductants MDA-MB231-shRAN1, -shRAN2 and -shRAN3 (Materials and methods). These 3 stably-transduced cell lines produced

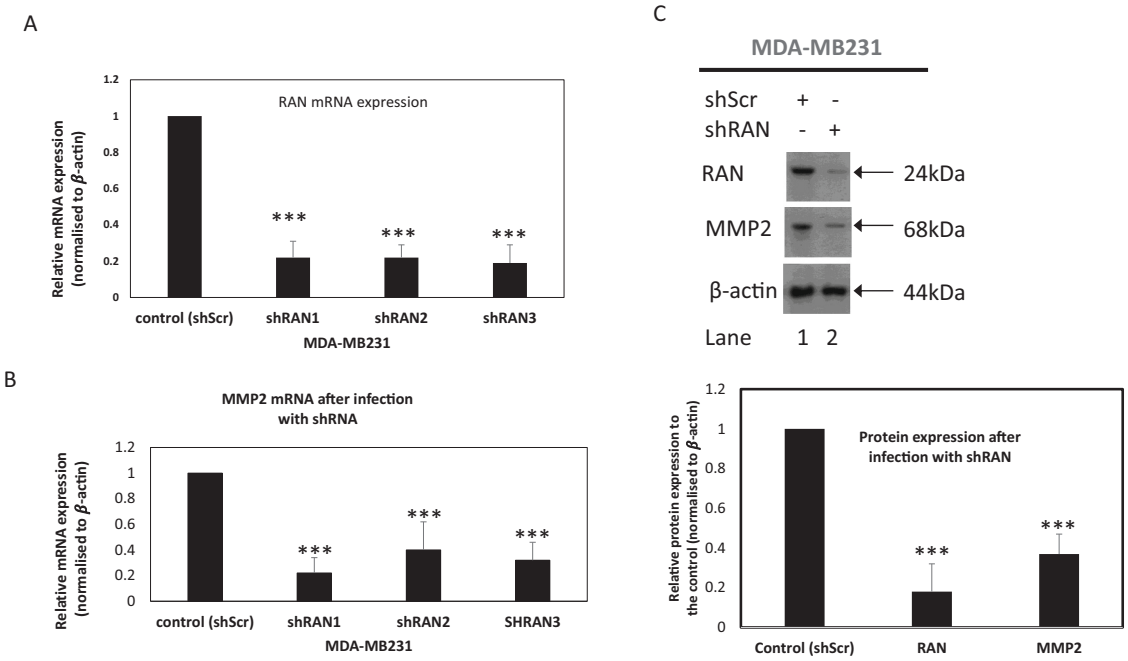

Fig. 1. Knockdown of RAN downregulates MMP2 in MDA-MB231 cell line. (A, B) MDA-MB231 breast cancer cell line was infected/transduced with either shScr or shRan, yielding MDA-MB231-shScr (shScr) or MDA-MB231-shRAN1, 2 or 3 cell lines (shRAN1, 2, 3) and relative mRNA levels were obtained from Real-Time PCR analysis for (A) RAN and (B) MMP2 and normalized to that of β-actin and then to control shScr cells (Materials and methods). Results are mean of three independent experiments ± SD. (C) Western blot for RAN, MMP2 and β-actin in the breast cancer cell line. Major immunoreactive bands are shown in kilodaltons (kDa). The average fold change for three different experiments for RAN normalized to β-actin and then to control shScr cells for RAN is in lane 1 = 1 and lane 2 = 0.18 ± 0.06 and for MMP2 is in lane 1 = 1 and lane 2 = 0.37 ± 0.1. The image shown is representative of the three experiments. The average fold decrease for three different experiments for RAN is 5.5 ± 0.6 and for MMP2 is 2.7 ± 0.3 compared to control shScr transduced cells.

reductions in RAN mRNA of 78 %, 79 % and 81 %, respectively compared to the MDA-MB231 cell line transduced with control scrambled shRNA, termed MDA-MB231-shScr (Fig. 1A, Student's *t*-test, $P = 0.0059$, $P = 0.0076$ and 0.0028, respectively). Three shRNA transduced cell lines, MDA-MB231-shRAN1, MDA-MB231-shRAN2 and MDA-MB231-shRAN3 (Materials and methods) were used to investigate the effect of lowering RAN mRNA on the regulation of a potential target matrix metalloproteinase 2 (MMP2). MDA-MB231-shRNA1, -shRNA2 and -shRNA3 contained levels of MMP2 mRNA reduced by 78 %, 60 % and 68 %, respectively, compared to MDA-MB231-shScr cells (Fig. 1B, $P = 0.0036$, $P = 0.016$ and $P = 0.0035$, respectively). Since the 3 shRAN transduced cell lines contained similar levels of RAN mRNA, we have used MDA-MB231-shRAN1 cells in the remainder of this study. Moreover Western blot analysis demonstrated that both RAN and MMP2 proteins were reduced in this shRAN transduced cell line by 5.5 fold and 2.7 fold respectively, compared to MDA-MB231-shScr cells (Fig. 1C, upper & lower panels; $P < 0.0001$).

3.2. Reduction of MMP2 expression by RAN knockdown reduces cell adhesion and invasion

In a previous study the 3 MDA-MB231-shRAN cell lines produced a significant decrease in cell adhesion and colony formation compared to control MDA-MB231-shScr cells [2,3,19]. When MDA-MB231 cells were transduced with shMMP2 to yield the MDA-MB231-shMMP2 cell line, it contained a significant decrease in MMP2 protein by 3.3 fold (Fig. 2A; upper & lower panels, $P = 0.0001$) and produced a significant decrease in cell adhesion by 52 % (Fig. 2B; Supplementary Fig. S2A, $P = 0.0012$), in colony formation by 68 % (Supplementary Fig. S2B, Fig. 2C; $P = 0.0005$) and in cell invasion by 62 % (Fig. 2D, $P = 0.0003$) compared to control MDA-MB231-shScr cells. When MDA-MB231 cells were transfected with an expression vector pBabe with the cDNA for MMP2, the resultant transfectant MDA-MB231-MMP2 contained a significant 2.1-fold higher level of MMP2 than in the control MDA-MB231(pBabe + shScr) vectors alone cell line ($P < 0.0001$) without affecting the level of RAN protein (Fig. 2E, left & right panels, $P = 0.07$). This elevated level of vector-produced MMP2 was also maintained in MDA-MB231-shRAN cells that had been subsequently transfected with pBabe expression vector for MMP2 ($P = 0.0001$), although these cells still contained a 3.0 fold reduction in level of RAN protein (Fig. 2E). When RAN levels were reduced in MDA-MB231-shRAN cells, there was a significant decrease in cell adhesion by nearly 60 % (Fig. 2F, $P = 0.003$) and invasion by 70 % compared to scrambled shRNA transfected cells (Fig. 2G, P = 0.0001). When MMP2 was overexpressed in MDA-MB231-shRan cells transfected with the expression vector for MMP2, there was a significant 62 % increase in cell adhesion (Fig. 2F, $P = 0.0009$) and a 73 % increase in cell invasion (Fig. 2G, $P = 0.0001$) compared to the untransfected MDA-MB231-shRAN cells, raising them up to similar levels produced by the original control MDA-MB231-shScr cells (Fig. 2F, G, $P = 0.07/P = 0.06$, respectively).

We then further investigated the importance of MMP2 in estrogen receptor α positive breast cancer cell lines, MCF-7 and T47D for proof of principle as to whether knockdown of MMP2 may also influence cell lines from another type of breast cancer. When MMP2 was knockdown in MCF-7 and T47D cell lines by transduction with shMMP2, they contained 3.9 fold (Fig. 3A, upper & lower panels, $P = 0.001$) and 2 fold (Fig. 3C, upper & lower panels, $P = 0.002$) lower levels of MMP2 and produced reductions in colony formation of 6.6 fold ($P = 0.003$) and 7.1 fold ($P = 0.0006$), respectively (Fig. 3B and D). These results suggest that expression of MMP2 is important for these breast cancer cell lines to maintain their tumorigenic properties in vitro. When the MCF-7-shRAN cells were transfected with the expression vector pBabe MMP2 cDNA, the resultant transfectants also produced a significant 2.9-fold increase in MMP2 protein ($P = 0.002$), similar to the level found in the MMP2 cDNA transfected control MCF-7 cells ($P = 0.5$), without any increase in the already depressed level of RAN (Fig. 3E, upper & lower panels).

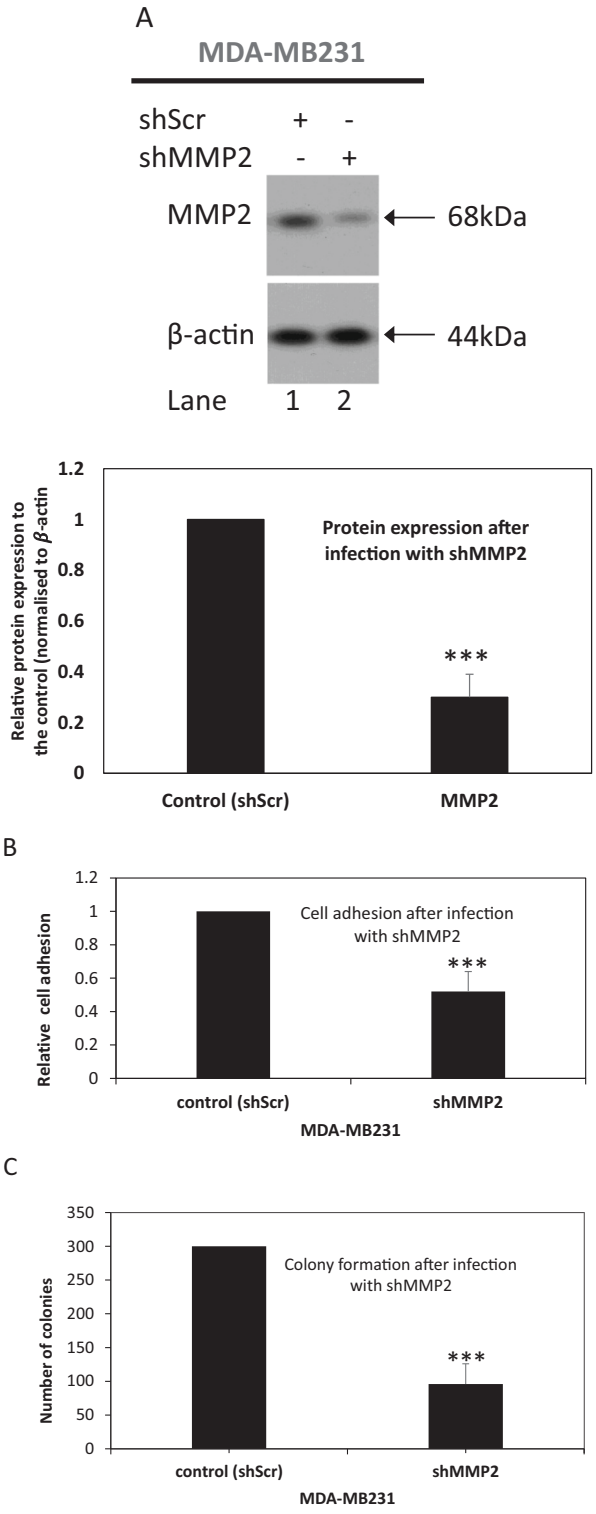

Fig. 2. Effect of MMP2 on in vitro biological properties associated with cancer progression in MDA-MB231 cells. (A, B, C,) MDA-MB231 breast cancer cells were infected/transduced with either control shScr or shMMP2 and subsequently assayed as follows. (A) Western blotted for MMP2 and β-actin. The average fold changes normalized to β-actin and then to control shScr cells for three different experiments for MMP2 is in lane 1 = 1 and lane 2 = 0.3 ± 0.2. (B) Cell adhesion, (C) Colony formation in soft agar and (D) Cell invasion. Cell adhesion was normalized to that in shScr cells which was set at 1; the numbers of colonies growing in agar are shown directly, and cell invasion was normalized to that in shScr cells (Materials and methods). Results are mean of three independent experiments ± SD. (E, F, G) Transductant control MDA-MB231-shScr and MDA-MB231-shRAN cells (Materials and methods) above were transfected with a control expression vector alone (pBabe) or with pBabe expression vector for MMP2 and subsequently assayed as follows. (E) Western blotted for MMP2, RAN, and β-actin. The average fold changes normalized to β-actin and then to control cells for three different experiments for MMP2 are in lane 1 = 1, lane 2 = 2.1 ± 0.2 and lane 3 = 1.8 ± 0.2 and for RAN are in lane 1 = 1, lane 2 = 1.02 ± 0.4, lane 3 = 0.34 ± 0.2. The images shown are representative of the three experiments. Major bands are shown in kilodaltons (kDa). (F) Cell adhesion assays and (G) cell invasion assays were conducted as described in Materials and methods and show means ± SD for three independent experiments normalized to that for control MDA-MB231-shScr cells.

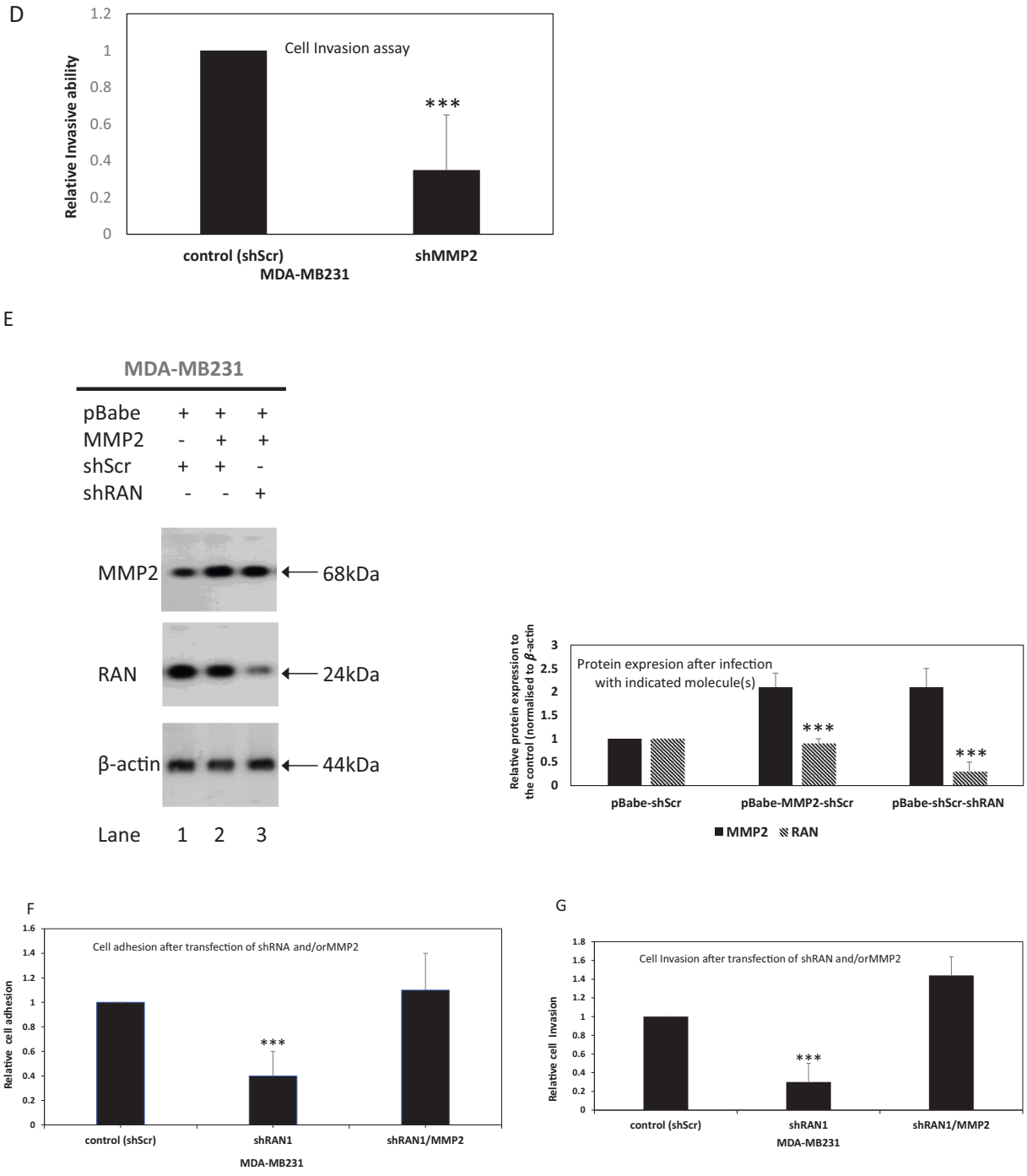

Fig. 2. (*continued*).

Similarly, the reduced level of colony-forming ability of the MCF-7-shRAN cells was increased 2.6-fold in these same cells after transfection with MMP2 cDNA ($P = 0.001$) to a level not significantly different from the control MCF-7-shScr cells transfected with pBabe vector alone (Fig. 3F, $P = 0.07$).These results with MDA-MB231 and MCF-7 cells showed that knockdown of RAN led to reduced colonising ability, but that this reduction could be overcome when the levels of MMP2 were raised, which suggests that RAN precedes MMP2 in this signalling pathway.

3.3. Mechanism of regulation of MMP2 by RAN

We next investigated whether silencing of RAN could lead to the down-regulation of MMP2's upstream regulatory genes of ATF3 [28] and/or CXCR3 [29] in RAN knocked down MDA-MB231cells. MDA-MB231-shRAN cells showed that levels of ATF3 and CXCR3 mRNAs both decreased significantly by 5.5 folds compared to those in the MDA-MB231-shScr control cell line (Fig. 4A, $P < 0.0001$). Western blots also demonstrated that silencing RAN by 2.9 folds led to a reduction in levels of ATF3, CXCR3 and MMP2 proteins by 2.8, 3.2, and 3.2-folds, respectively, in MDA-MB231-shRAN cells compared to control MDA-MB231-shScr cells (Fig. 4B, upper & lower panels; $P < 0.0001$). When CXCR3 was silenced in MDA-MB231-shCXCR3 transduced cells, CXCR3 mRNA decreased by nearly 7-fold (Fig. 4C, $P = 0.0006$), but there was no significant change in ATF3 mRNA ($P = 0.06$) (Fig. 4C). Similarly, when CXCR3 was silenced in MDA-MB231-shCXCR3 transduced cells, the

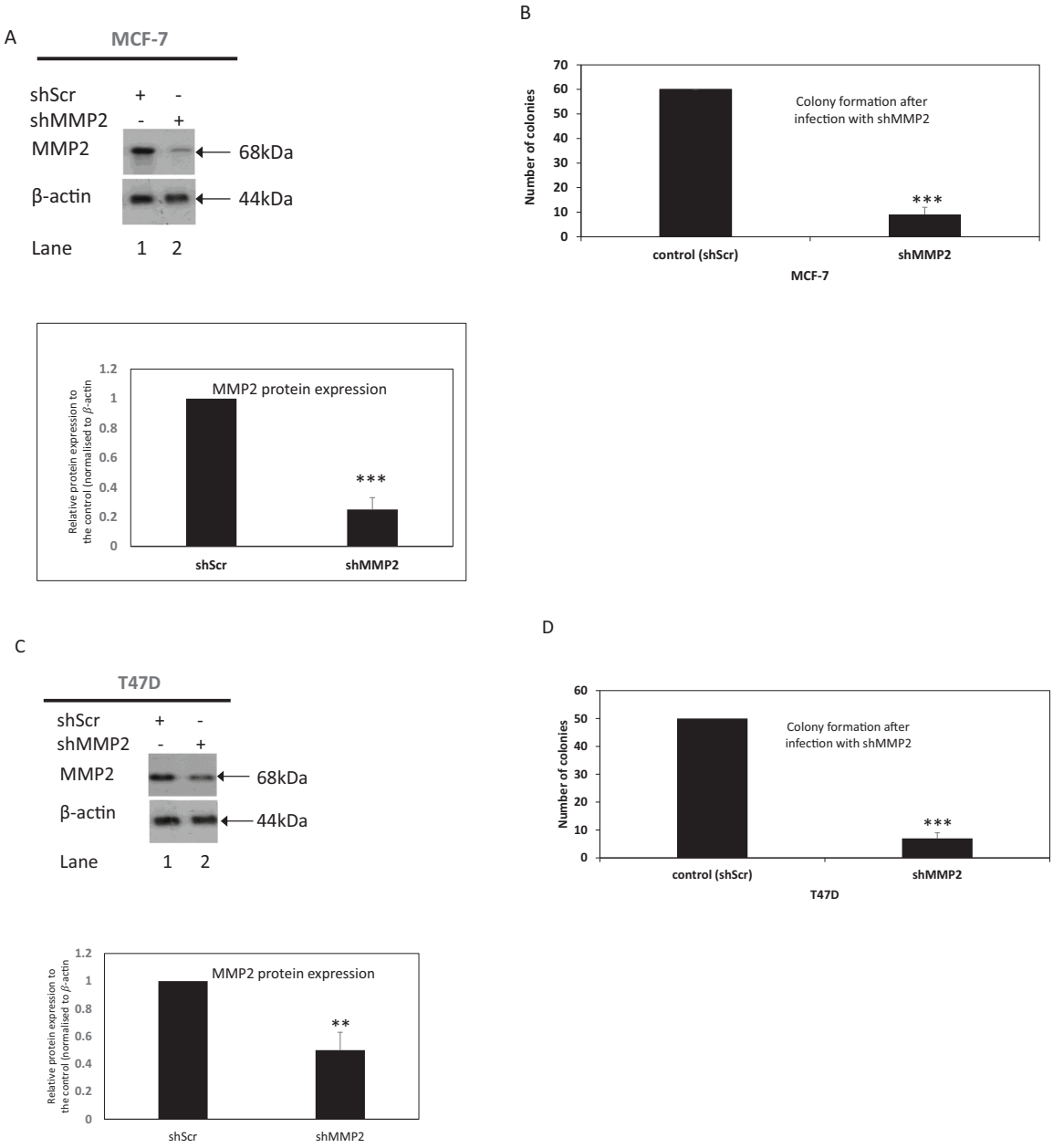

Fig. 3. Knockdown of MMP2 reduces growth in agar in MCF-7 and T47D breast cancer cell lines. (A, B) MCF-7 or (C, D) T47D breast cancer lines were infected/transduced with either shScr or shMMP2 and subsequentially assayed as follows. (A, C) Western blotted for MMP2 and β-actin showing a representative blot of three experiments. The average fold decrease for three experiments relative to shScr cells for MMP2 is (A) 3.9 ± 0.4, (C) 2.0 ± 0.2. (B, D) Colony formation in soft agar showing mean numbers ± SD of growing colonies from 3 experiments. (E, F) Control MCF-7-shScr and MCF-7-shRAN cells were transfected with pBabe or pBabe expression vector for MMP2 and assayed as follows. (E) Western blotted. The images shown are representative of three experiments. The average fold changes relative to control shScr cells for three different experiments are for MMP2 in lane 1 = 1, in lane 2 = 2.9 ± 0.3, in lane 3 = 2.8 ± 0.3 and in lane 4 = 3.0 ± 0.4 and for RAN in lane 1 = 1, in lane 2 = 1.2 ± 0.05, in lane 3 = 1.2 ± 0.06 and in lane 4 = 2.7 ± 0.3 (F) Colony formation in soft agar showing mean numbers ± SD of growing colonies from three independent experiments.

MMP2 protein decreased by 3.2-fold (Fig. 4D, $P = 0.003$), but there was no significant change in ATF3 protein level (Fig. 4D, upper & lower panels $P = 0.06$). In contrast when ATF3 mRNA was silenced in MDA-MB231-shATF3 transduced cells by about 7-fold ($P = 0.0004$), there was a significant decrease in both MMP2 and CXCR3 mRNA levels by 60 % ($P = 0.001$) and 67 % ($P = 0.0008$), respectively, compared to control MDA-MB231-shScr cells (Fig. 4E). Similarly silencing ATF3 led to reduced levels of ATF3, CXCR3 and MMP2 proteins by 2.8, 3.0, and 2.4-folds respectively, in MDA-MB231-shATF3 transduced cells compared to control MDA-MB231-shScr cells (Fig. 4F, upper & lower panels; $P < 0.0001$). Moreover, both the colony-forming ability and the ability of MDA-MB231 cells to invade, the properties most closely associated with metastasis [30] were reduced by 80 % (Fig. 4G, $P = 0.001$) and 77 % (Fig. 4H, $P = 0.001$), respectively for MDA-MB231-shCXCR3 transduced cells and by 2.8-fold (Fig. 4I, $P = 0.006$) and 2.5-fold (Fig. 4J, $P = 0.002$), respectively for MDA-MB231-shATF3 transduced cells over control MDA-MB231-shScr cells. These results suggest that a reduction in RAN probably reduces MMP2, at least in part, by reducing firstly ATF3 and then CXCR3, and that the latter two proteins also lie on the pathway that signals increases in cellular properties associated with metastasis.

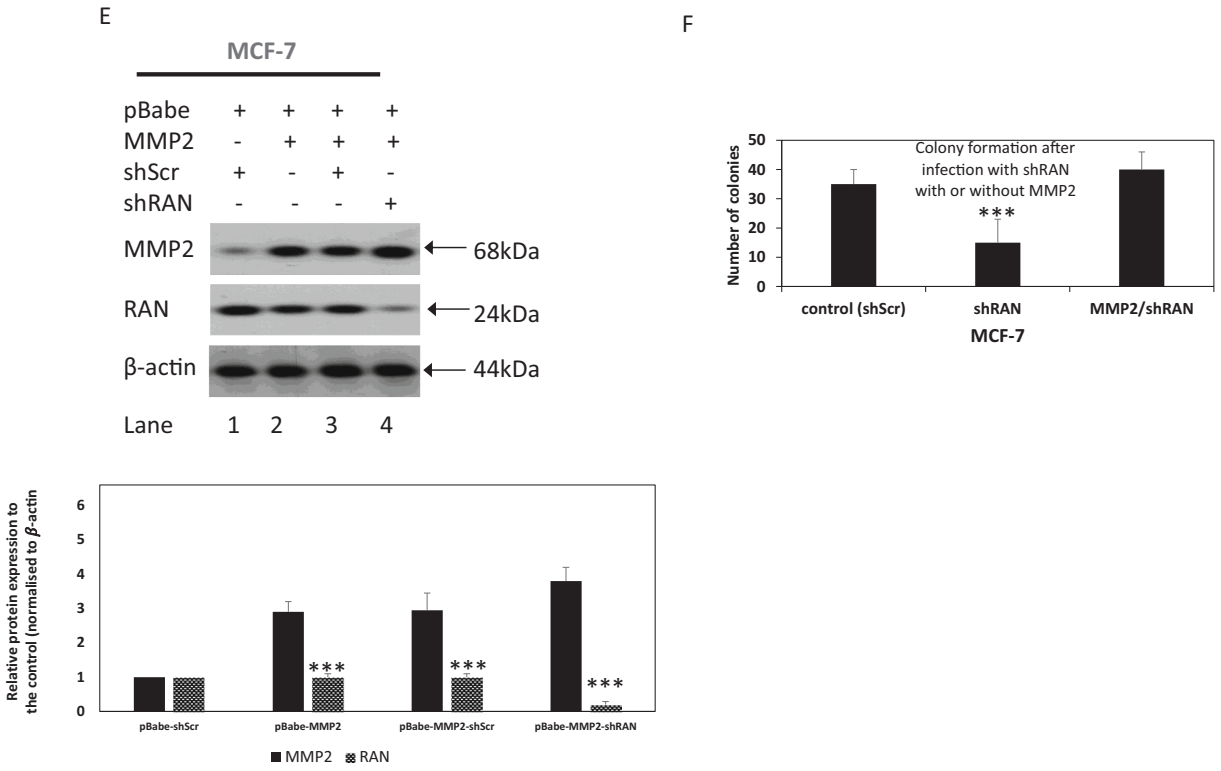

Fig. 3. (*continued*).

3.4. Association of RAN-related molecules with patient survival times in human breast cancer

Next, we investigated the relationship in human breast cancer between RAN and other potential downstream markers including MMP2 with patient demise, probably as a result of metastasis [31]. To simplify subsequent statistical analyses, the individual carcinoma cell staining groups for each protein were separated into two categorical groups using previously determined cut-offs of 1 % or 5 % to separate those which were the most significantly different in patient survival times (Materials & Methods). The largest significant differences in relative risk (RR) in this group of 181 patients were as follows:

RAN ($\chi^2 = 35.4$, RR = 14.9), cMet ($\chi^2 = 32.9$, RR = 10.7), cMyc ($\chi^2 = 40.3$, RR = 9.5), MMP2 ($\chi^2 = 64.8$, RR = 7.7) and CK5/6 ($\chi^2 = 43.3$, RR = 5.6) (Supplementary Table S3). Stainings for ERα ($\chi^2 = 1.24$, RR = 0.81), c-erbB-2 ($\chi^2 = 1.93$, RR = 1.33) and Ki67 ($\chi^2 = 1.6$, RR = 1.3) were not significantly different in this group of patients, although they were significant in a larger patient group [32]. By comparison this group of patients either with or without tumour involvement of lymph nodes showed a significant RR of 2.3 ($\chi^2 = 14.64$, 1df, $P < 0.001$), those groupings based on tumour size and histological grade were not significantly different (Supplementary Table S3).

3.5. Association of RAN and target molecules in primary breast tumours

Results of IHC staining in primary tumours for RAN and its relationship with that of other molecular tumour markers showed that RAN was very significantly associated with c-Met($P = 6.6 \times 10^{-5}$), cMyc ($P = 4.4 \times 10^{-5}$), MMP2 ($P = 5.7 \times 10^{-6}$), and CK5/6 ($P = 5.5 \times 10^{-5}$), but not at all with Ki67, ERα, c-erbB-2, tumour size and histological grade ($P \geq 0.94$) and only of possible borderline significance with TRNBC (P uncorrected = 0.06) and involved lymph nodes alone (P uncorrected = 0.037). The most significant association of staining for RAN was with that for MMP2 ($P = 5.7 \times 10^{-6}$) (Supplementary Table S4). When staining for MMP2 was tested for its relationship with staining for the other tumour variables, it was significantly strongly associated with the same variables as RAN: cMet ($P = 6.4 \times 10^{-9}$), cMyc ($P = 1.8 \times 10^{-7}$), CK5/6 ($P = 7.5 \times 10^{-7}$), as well as with RAN itself ($P = 5.7 \times 10^{-6}$). The other tumour variables were not significantly associated with MMP2 ($P \geq 0.35$) (Supplementary Table S4).

When staining for RAN was tested for its relative probability of association (RA) with that of its potential target molecules cMet, cMyc, MMP2 and Ki67 using binary logistic regression, the RAs with cMet and MMP2 were significant and the strongest (RA = 3.0 to 3.4), but that with Ki67 was not significant (RA = 1.12, $P = 0.81$) (Table 1). Moreover, when staining for c-Met was analysed, it also showed the strongest associations with that for RAN (RA = 3.41, $P = 0.019$) and for MMP2 (7.9, $P < 0.001$), but the strongest association for cMyc was with MMP2 (RA = 5.2) and that for MMP2 was with cMet (RA = 7.7) (Table 1), suggesting a closer association between these 3 molecules than with RAN itself in the primary tumours.

3.6. Association of RAN, MMP2 and patient survival

When staining for RAN, cMet, cMyc and MMP2 (Supplementary Fig. S3) were tested together for independent association with patient survival times using Cox's multivariate analysis, they all showed some significant degree of independence ($P \leq 0.036$) with similar relative risks (RR) for patient demise of 3.1 to 3.7 fold (Table 2). These RRs were considerably less than the 7 to 15-fold decreases obtained in univariate analyses (Supplementary Table S3). When analysed in binary combinations of staining for RAN with that for cMet, for cMyc or for MMP2, the RR for patient demise was suppressed from 14.9 to 7.6–7.8 fold for RAN with cMet or with MMP2, but only to 9.8 fold with cMyc (Table 2), these results suggested that RAN was more closely related to the former 2 proteins cMet and MMP2 in its association with patient demise. However, the effects of staining for RAN and for MMP2 on RR were synergistic, increasing from 17.1 and 23.1, respectively, to 82.1 (Supplementary Table S5) or, in terms of patients surviving, from 64 % and 60 %, respectively, to only 6 % surviving after nearly 20 years (Fig. 5).

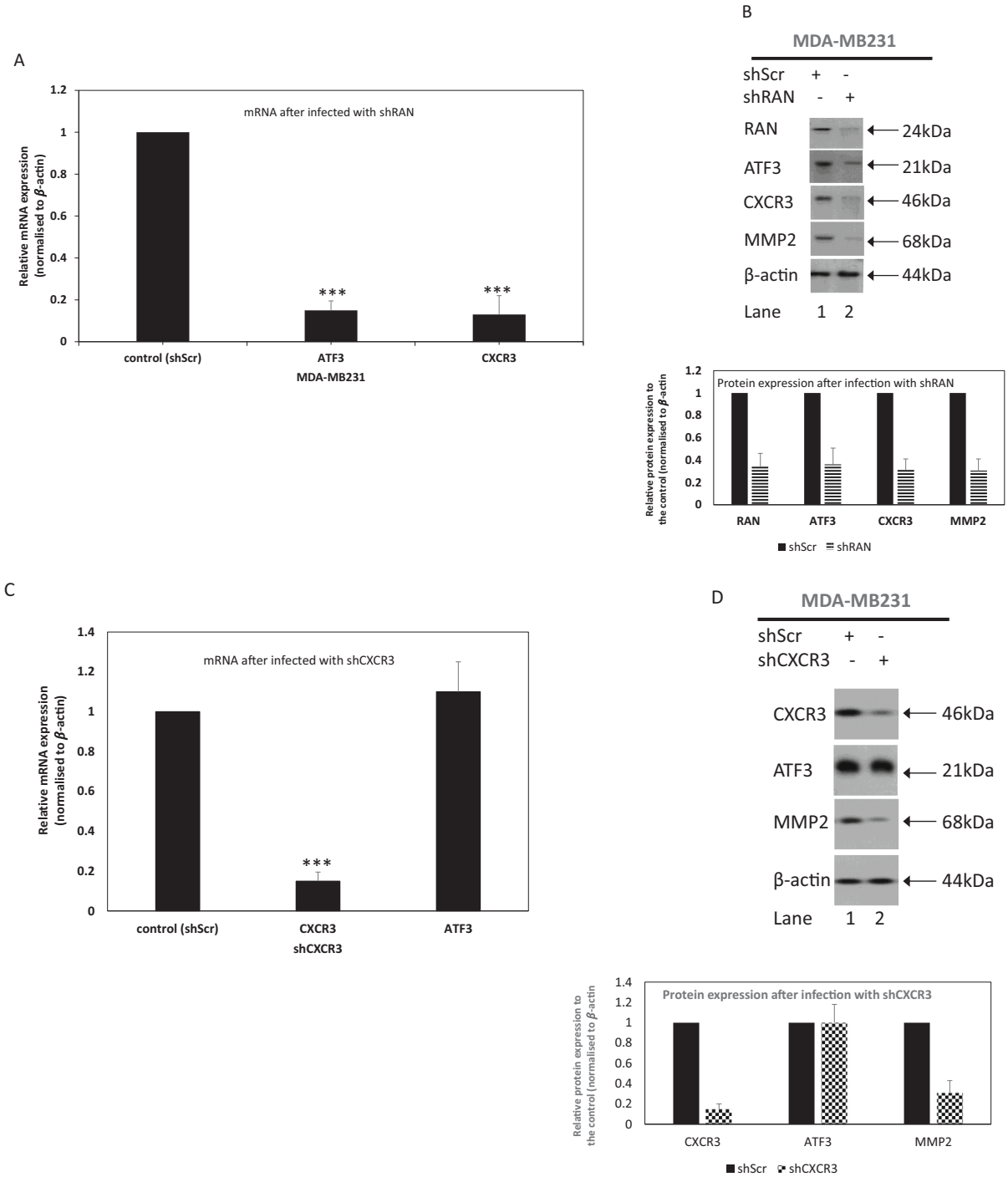

Fig. 4. Mechanism of dysregulation of MMP2 in breast cancer cells. MDA-MB231 breast cancer cells were infected/transduced with (A, B) either shScr or shRAN; with (C, D, G, H) either shScr or shCXCR3; and with (E, F, I, J) either shScr or shATF3 and then assayed as follows. (A) RT-PCR for mRNAs for ATF3 and CXCR3. Levels of mRNAs are shown as means ± SD for three independent experiments relative to β-actin mRNA and then normalized to the control shScr cell values for the specific mRNA. (B) Western blotted for proteins for RAN, ATF3, CXCR3, MMP2, β-actin. The average fold reduction relative to control shScr cells for three different experiments for RAN protein is in lane 1 = 1 and lane 2 = 2.9 ± 0.09, for ATF3 is in lane 1 = 1, lane 2 = 2.8 ± 0.1, for CXCR3 is in lane 1 = 1 and lane 2 = 3.2 ± 0.07 and for MMP2 is in lane 1 = 1 and lane 2 = 3.2 ± 0.5 (C) RT-PCR for mRNAs for CXCR3 and ATF3. Levels of mRNAs are shown as means ± SD for three independent experiments relative to β-actin mRNA and then normalized to the control shScr values for the specific mRNA. (D) Western blotted for proteins for CXCR3, ATF3, MMP2 and β-actin. The average fold change relative to control shScr cells for three different experiments ± SD for CXCR3 is in lane 1 = 1 and lane 2 = 0.37 ± 0.0.05, for ATF3 is in lane 1 = 1, lane 2 = 0.10 ± 0.04 and for MMP2 is in lane 1 = 1 and lane 2 = 0.32 ± 0.04. (E) RT-PCR for mRNAs for ATF3, CXCR3 and MMP2. Levels of mRNAs are shown as means ± SD for three independent experiments relative to β-actin mRNA and then normalized to the control shScr cell values for the specific mRNA. (F) Western blotted for ATF3, CXCR3, MMP2 and β-actin. The average fold change relative to control shScr cells for three different experiments for ATF3 is in lane 1 = 1 and lane 2 = 0.35 ± 0.03, for CXCR3 is in lane 1 = 1, lane 2 = 0.33 ± 0.06 and for MMP2 is in lane 1 = 1 and lane 2 = 0.41 ± 0.06. (G,I) Colony formation in soft agar and (H, J) cell invasion; both sets of results were normalized to those obtained in control shScr cells which were set at 1 and are the means of three independent experiments ± SD.

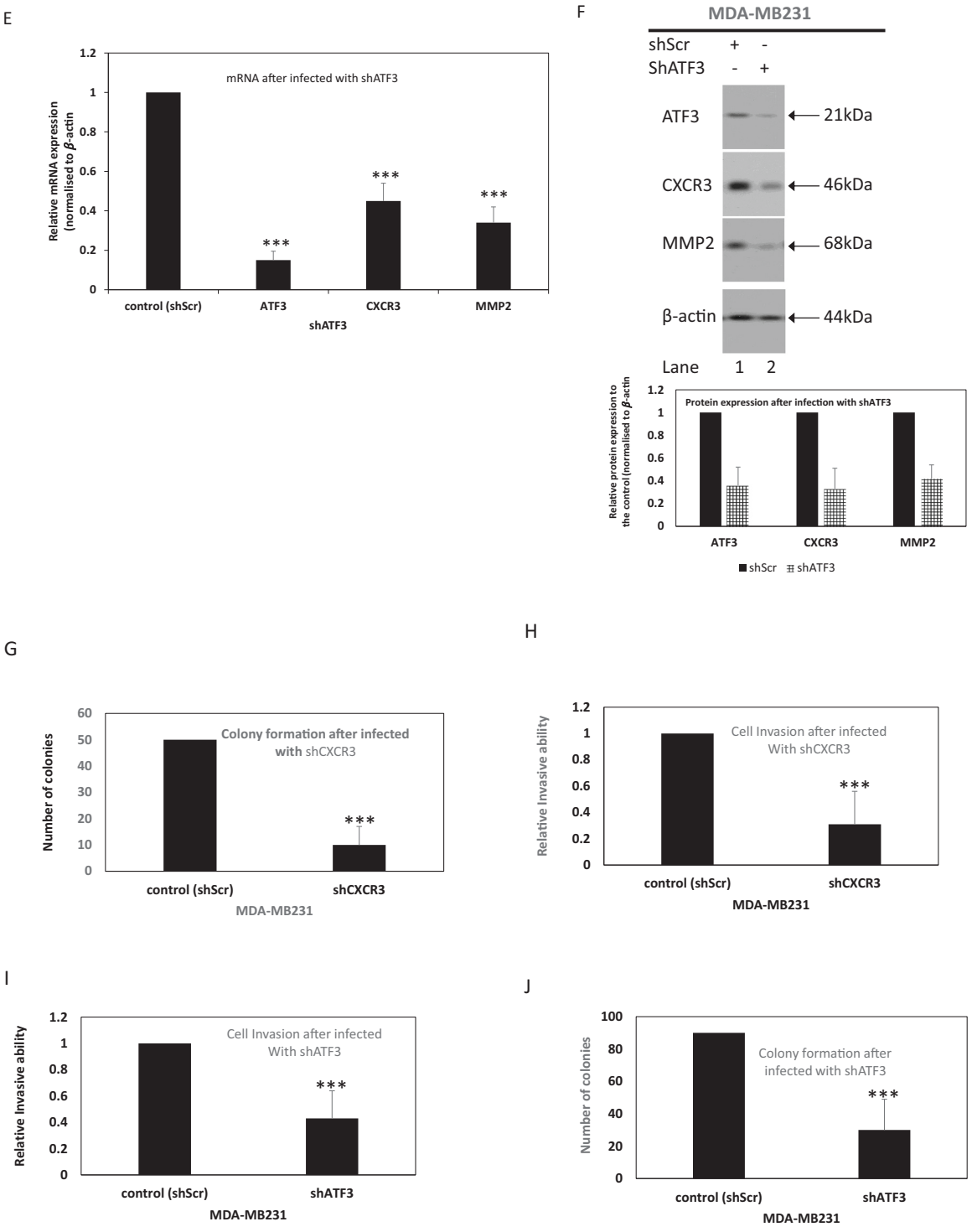

Fig. 4. (*continued*).

Moreover, there was a significant decrease in patient survival times for the doubly stained RAN+MMP2+ over the single-stained RAN+MMP2- group ($P < 0.001$), but not over the RAN-MMP2+ group ($P = 0.21$) (Supplementary Table S5).The sensitivity, specificity, positive predictive response (PPR) and negative predictive response (NPR) of IHC scoring for RAN or MMP2 alone and for RAN with MMP2 are presented in Table 3. The NPR is shown to the best for the two biomarkers RAN and MMP2 taken together than when one of them is used alone for the prediction of patients alive (Table 3).

3.7. Association of IHC staining for RAN and for MMP2 with overall time of patient survival for ERα positive and ERα negative patients

Since breast cancer patients are often separated for treatment purposes into ERα positive and ERα negative groups [33], we investigated the effect of RAN or MMP2 alone and in combination with time of survival of patients with ERα positive and with ERα negative breast tumours. Patients with either RAN or MMP2 positively-staining tumours still demonstrated significantly shorter survival times than those with RAN or MMP2 negatively-staining tumours in either ERα positive or ERα

Table 1
Probability of independent association of staining for RAN and other molecular markers.

Test[a] variable	Other[b] variables	Coeff β[c]	SE of β[c]	χ^2 [d]	P[e]	RA[f]	95 % CI[f]
RAN	cMet	1.221	0.536	5.185	0.023	3.39	1.19–9.69
	cMyc	0.677	0.521	1.687	0.194	1.97	0.71–5.47
	MMP2	1.099	0.628	3.064	0.080	3.00	0.88–10.27
	Ki67	0.117	0.493	0.056	0.813	1.12	0.43–2.96
cMet	RAN	1.228	0.525	5.462	0.019	3.41	1.22–9.56
	cMyc	0.866	0.498	3.018	0.082	2.38	0.90–6.31
	MMP2	2.067	0.566	13.327	<0.001	7.9	2.60–23.96
	Ki67	0.488	0.484	1.015	0.314	1.63	0.63–4.21
cMyc	RAN	0.697	0.515	1.833	0.176	2.01	0.73–5.50
	cMet	0.852	0.504	2.856	0.091	2.34	0.87–6.30
	MMP2	1.644	0.550	8.923	0.003	5.18	1.76–15.22
	Ki67	0.079	0.469	0.029	0.866	1.08	0.43–2.72
MMP2	RAN	0.982	0.627	2.451	0.117	2.67	0.78–9.13
	cMet	2.047	0.571	12.869	<0.001	7.74	2.53–23.70
	cMyc	1.587	0.553	8.238	0.004	4.89	1.65–14.46
	Ki67	0.305	0.468	0.424	0.515	1.36	0.54–3.40

[a] Principle IHC-staining variable for probability of association with other tumour variables using cut-offs defined in Materials and methods.
[b] Sets of other IHC-staining variables were included in binary Logistic Regression Analysis using cut-offs defined in Materials and methods to separate positive and negative staining groups.
[c] Value of coefficient β (Coeff β) with its standard error (SE) in binary Logistic Regression Analysis (Materials and methods).
[d] Logistic Regression statistic χ^2.
[e] Probability of association with test variable from Logistic Regression statistic χ^2 in each case.
[f] Relative Association (RA) and 95 % confidence interval (95%CI) from binary Logistic Regression Analysis.

Table 2
Summary of results for Cox's proportional hazards for cancer-related deaths.

Tumour variable[a]	Coeff β[b]	SE of β[b]	X^2 [c]	P[d]	RR[e]	95 % CI[e]
Set A						
RAN	1.305	0.622	4.398	0.036	3.69	1.09–12.49
cMet	1.153	0.503	5.257	0.022	3.17	1.18–8.49
cMyc	1.246	0.445	7.827	0.005	3.48	1.45–8.32
MMP2	1.127	0.310	13.225	<0.001	3.10	1.68–5.67
Set B						
RAN	2.025	0.594	11.600	0.001	7.57	2.36–24.28
cMet	1.985	0.470	17.879	<0.001	7.28	2.90–18.27
Set C						
RAN	2.286	0.592	14.918	<0.001	9.84	3.08–31.39
cMyc	1.873	0.427	19.252	<0.001	6.51	2.82–15.02
Set D						
RAN	2.056	0.600	11.727	0.001	7.82	2.41–25.36
MMP2	1.642	0.260	40.023	<0.001	5.17	3.11–8.59

[a] In Set A comparisons were made between duration of survival time of patients with tumours stained for Ran, cMet, cMyc and MMP2; overall $\chi^2 = 96.21$, 4df, $P < 0.001$. In Set B comparisons between patients with tumours stained for Ran and cMet; overall $\chi^2 = 52.4$, 2df, $P < 0.001$. In Set C comparisons between patients with tumours stained for RAN and cMyc; overall $\chi^2 = 60.6$, 2df, $P < 0.001$. In Set D comparisons between patients with tumours stained for RAN and MMP2; overall $\chi^2 = 96.5$, 2df, $P < 0.001$. IHC cut-offs as described in Materials and methods.
[b] Value of β coefficient (=$\log_e$RR) and standard error (SE) in Cox's multiple regression analysis (Materials and methods).
[c] Cox's statistic χ^2.

negative cases (Supplementary Fig. S1, Wilcoxon Gehan $P < 0.001$). In both ERα positive and ERα negative subgroups, patients with primary tumours staining for RAN and for MMP2 had significantly shorter survival times than those patients with tumours staining for RAN alone ($P <$ or $= 0.001$, respectively) increasing the RR by 5.9 fold (Cox's univariate analysis) in ERα positive and by 3.5 fold in ERα negative subgroups (Supplementary Fig. S1).Thus patients with RAN and MMP2 positively-staining tumours were also significantly associated with poorer survival times than those patients with only RAN positive tumours, whether or not they were diagnosed with ERα positive or negative tumours (Supplementary Fig. S1).

4. Discussion

Previously, we have shown that knockdown of RAN by shRNA results in reduction of in vitro cell biological properties including cell adhesion, colony formation and cell invasion [2,3,19], as well as in vivo metastasis [7]. Here RAN knockdown in breast cancer cells reduces MMP2 mRNA and protein levels, probably via ATF3 and CXCR3 which, in turn, results in a significant reduction in cell adhesion and colony formation in breast cancer cell lines. However, overexpression of MMP2 in RAN knocked-down breast cancer cells results in overcoming RAN silencing and this leads to increases in cell adhesion and cell invasion. The fact that transfection of pBabe MMP2 overcomes the knockdown effect of RAN on the levels of MMP2 and consequent biological effects is probably due to the natural promoter being different from that of pBabe for MMP2. However, we have not observed a substantial rise over the control cells (Fig. 2F & G). This may be due to RAN only partially mediating its effects on cell adhesion and colony formation via MMP2, but it may also exert its effect via other target genes. Previously, we have shown that RAN's action can be mediated through c-Met [19] and osteopontin [2], in addition to Met-driven activation of cell adhesion, migration, and invasion. To identify the other target genes implicated in the RAN pathway, we are currently undertaking RNA microarray analysis on shRAN-infected cells in comparison to shScr control cells.

Although previous studies have shown that protein degrading enzymes such as the MMPs contribute to tumour progression, invasion and metastasis [34,35], their role in adhesion has been relatively confusing because of the different assays used. Here we show that reducing MMP2 in MDA-MB231 cells reduces their adhesion to fibronectin-coated plastic surfaces and that it also decreases their colony-forming ability in a semisolid medium of agar. The former is a measure of heterotypic adhesion to the extracellular matrix (ECM) and the latter a loss of homotypic cell-cell adhesion to each other. Thus in our hands a reduction in MMP2 reduces heterotypic adhesion but increases homotypic adhesion, in broad agreement with this field [36]. In cancer cells, adhesion to the ECM and to each other is largely controlled by integrins and E-cadherin, repectively [37], and it is possible that MMP2 can interact, either directly or indirectly with either set of adhesive proteins. For example in human melanoma cells, MMP2 cuts fibronectin into small fragments to stimulate heterotypic adhesion mediated by $\alpha_v\beta_3$ integrin [38] and it acts similarly in ovarian cancer cells [39], the latter response can be inhibited using siRNAs or blocking-antibodies to MMP2

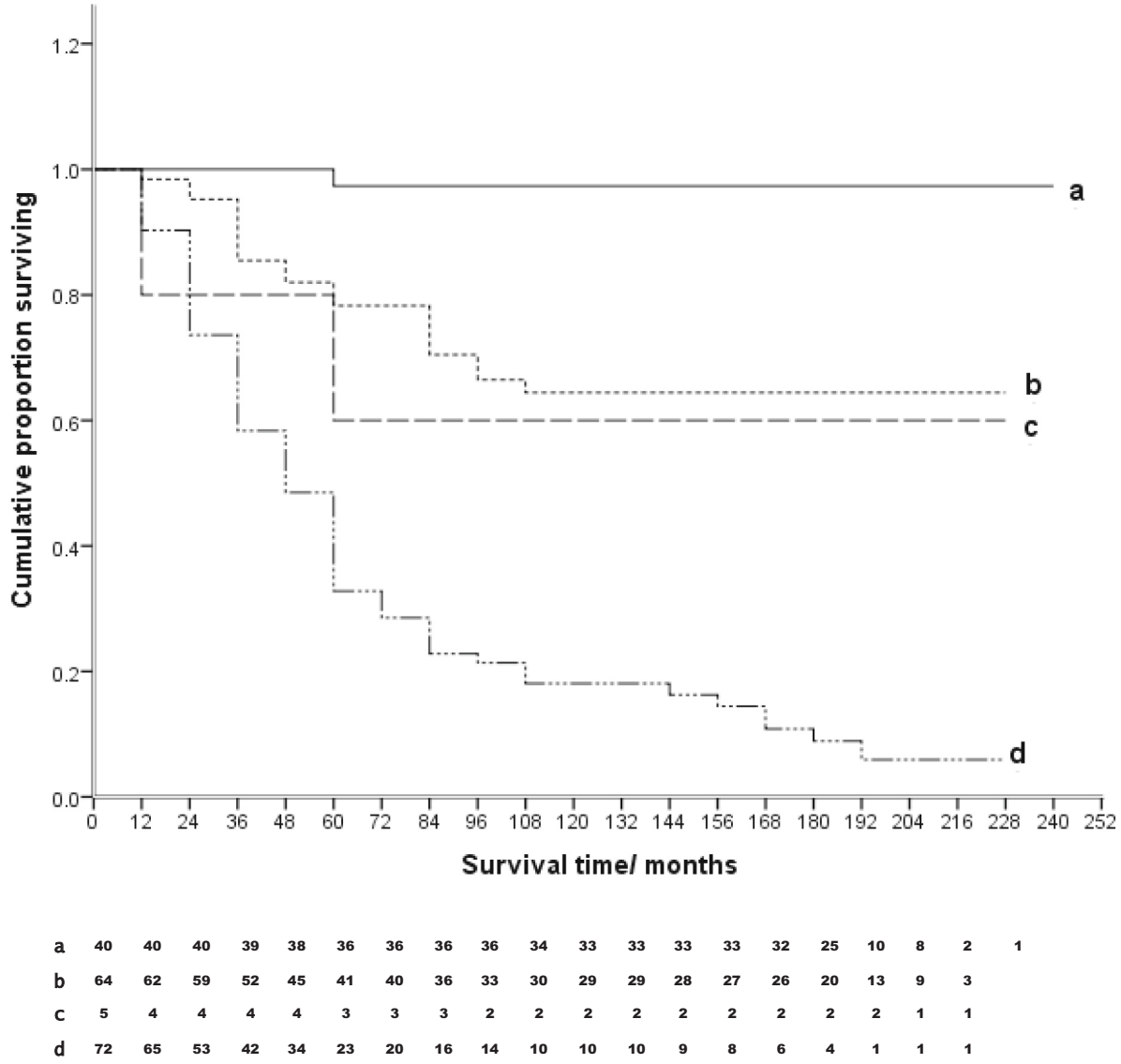

a	40	40	40	39	38	36	36	36	36	34	33	33	33	33	32	25	10	8	2	1
b	64	62	59	52	45	41	40	36	33	30	29	29	28	27	26	20	13	9	3	
c	5	4	4	4	4	3	3	3	2	2	2	2	2	2	2	2	2	1	1	
d	72	65	53	42	34	23	20	16	14	10	10	10	9	8	6	4	1	1	1	

Fig. 5. Association of IHC staining for RAN and for MMP2 with overall time of patient survival. Cumulative proportion of surviving patients as a fraction of the total for each year after presentation with carcinomas classified as negatively stained for RAN (−) and MMP2 (−) (**set a** solid line), positively stained for RAN (+) and negatively stained for MMP2 (−) (**set b** dotted line), negatively stained for RAN (−) and positively stained for MMP2 (+) (**set c** dashed line), and positively stained for both RAN (+) and MMP2 (+) (**set d** dashed and dotted line). Numbers of patients entering each year are shown below. In **a** median survival (ms) >228 months, final cumulative survival (fcs) 0.97 with 39 censored observations (8 dead of other causes); in **b** ms >216 months, fcs 0.6 with 44 censored observations (19 dead of other causes); in **c** ms >216 months, fcs 0.60, with 3 censored observations (1 dead of other causes) and in **d** ms 46.2 months, fcs 0.06, with 8 censored observations (4 dead of other causes). The 4 curves are highly significantly different (Wilcoxon Gehan statistic $\chi^2 = 75.405$, 3 df, $P < 0.001$). For **a vs b** Wilcoxon $\chi^2 = 14.02$, 1 df, $P < 0.001$, Cox's univariate RR = 17.11 (95 % CI, 2.30–127.6); **a vs c** $\chi^2 = 10.583$, $P < 0.001$, RR = 23.10 (2.09–255.0); **b vs c** $\chi^2 = 0.407$, $P = 0.52$, RR = 1.35 (0.32–5.78); **b vs d** $\chi^2 = 33.09$, $P < 0.001$, RR = 4.8 (2.88–7.99); **c vs d** $\chi^2 = 1.569$, $P = 0.21$, RR = 3.56 (0.87–14.61); **a vs d** $\chi^2 = 59.64$, $P < 0.001$, RR = 82.11 (11.34–594.6).

[40]. In contrast, in human nasopharyngeal carcinoma cells MMP2 reduces expression of E-cadherin and homotypic cell-cell adhesion [41] and suppression of Friend leukemia virus integration 1 in hepatocellular carcinoma cells reduces MMP2 and the cells' colony-forming ability [42], thereby increasing their homotypic adhesion.

In this study, knockdown of CXCR3 results in reduction of mRNA/protein levels of MMP2 with no changes in ATF3 expression. However, silencing of ATF3 causes a reduction in both MMP2 and CXCR3 mRNA/protein expression (Fig. 4).Thus, it is probable that the RAN/MMP2 pathway is connected in the order of RAN → ATF3 → CXCR3 → MMP2 and this leads onto the cellular properties associated with metastasis (Fig. 6). It has been established that CXCR3 is suppressed in cardiomyocytes and macrophages from ATF3-knockout mice and is positively upregulated by ATF3 through an ATF3 transcriptional response element found in its proximal promoter [43]. In another study, knockdown of ATF3 using siRNA reduced the expression of MMP2 and inhibited the growth of U373MG cells grown in vivo xenografts in nude mice [14]. It has also been shown that CXCR3 promotes gastric cancer cell migration and invasion by upregulating MMP2 expression [27]. Our results are consistent with these reports.

Although previous publications [2,3,19] and work in this paper have established a causal relationship between RAN, cMet, cMyc on the one hand and with RAN, MMP2 on the other hand and with properties related to metastasis, these studies have been undertaken in cell line models of breast cancer. By using IHC staining of primary breast cancers, we have also previously shown that RAN [2], cMet [19], and cMyc [3]

Table 3
Sensitivity, specificity, NPR and PPR for Ran and MMP-2 (IHC assay).

Breast cancer Sub-type	IHC assay	IHC staining score at diagnosis of BC	Patients alive[a]		Patients died from cancer[b]		Total patients		Sensitivity (true +ve rate)	Selectivity (true −ve rate)	PPR[c]	NPR[d]
			No.	% Alive	No.	% Died	No.	% Total	%	%	%	%
All	RAN (Nuc)	<1 % (−ve)	42	44.7	3	3.4	45	24.9		44.7		93.3
All	RAN (Nuc)	2 to 5 % (+ve)	52	55.3	84	96.6	113	75.1	96.6		74.3	
All	RAN (Nuc)	Total	94	100	87	100	181	100				
All	MMP2	<2 % (−ve)	83	88.3	21	24.1	104	57.5		88.3		79.8
All	MMP2	2 to 5 % (+ve)	11	11.7	66	75.9	77	42.3	75.9		91.7	
All	MMP2	Total	94	100	87	100	181	100				
All	RAN(Nuc)/ MMP2	−ve/−ve	39	41.0	1	1.1	40	22.1		41.0		97.5
All	RAN(Nuc)/ MMP2	All others	47	50.0	22	25.3	69	38.1				
All	RAN(Nuc)/ MMP2	+ve/+ve	8	8.5	64	73.6	72	39.8	98.9		88.8	
All	RAN(Nuc)/ MMP2	Total	94	100	87	100	181	100				

[a] Patients monitored up to 20 years from diagnosis and free from radiotherapy, chemotherapy and hormone therapy.
[b] Cases of death by other causes have been excluded.
[c] PPR = positive percentage response.
[d] NPR = negative percentage response

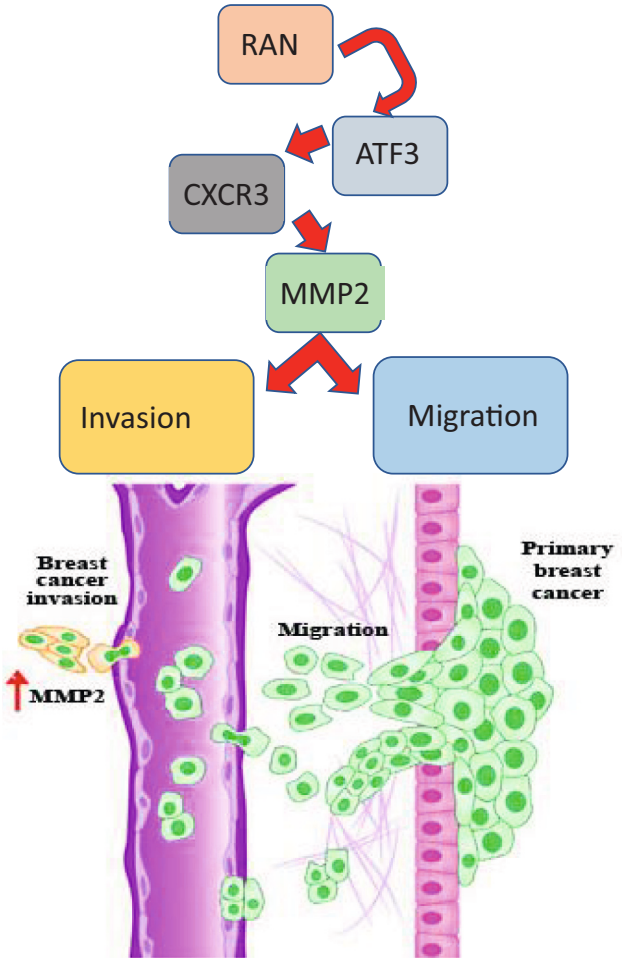

Fig. 6. Effector model for RAN pathway.
RAN induces ATF3 and then CXCR3 which, in turn stimulates production of MMP2. MMP2 protein functions as positive RAN effector that stimulates cell migration, cell invasion and eventually metastasis in breast cancer cells.

are on their own significantly associated with patient demise from metastatic breast cancer. Now we have shown that increased staining for RAN in these primary tumours is very significantly associated with staining for these same proteins cMet, cMyc, and MMP2. Since increased IHC staining is related to increased levels of protein in the carcinoma cells [2], protein levels have also therefore increased by similar levels of at least 5–10 folds between tumours whose patients are at low and those who are at high risk of dying from metastatic disease. These fold increases in cellular levels are sufficient to cause the increases in metastatic properties observed in stably-transfected cells in culture as outlined above. There is no significant association of staining for RAN with that for Ki67, consistent with little increase in cell proliferation being observed in RAN transfected cells. The fact that staining for RAN [2], MMP2 (Supplementary Table S4) and cMet [2,19], cMyc [3] are all very significantly associated with that for CK5/6, but not with that for ERα or c-erbB-2 suggests that these proteins occur mainly in the Basal Cell Type of breast cancers. This subgroup of breast cancers overlaps considerably with the triple receptor negative breast cancer (TRNBC) group [26,27] and hence may explain the observed borderline association of staining for RAN with the TRNBC subgroup alone (Supplementary Table S4). The fact that there is a stronger relative association (RA) between staining for MMP2, cMet and cMyc than with that for RAN (Table 1) suggests that the increase in MMP2 in tumours is not solely due to an increase in RAN, but may arise via other signalling mechanisms.

Multiple longitudinal comparisons of survival times with RAN, cMet, cMyc and MMP2 in multivariate analyses showed that all 4 were independently significantly associated with patient survival times, but that either together with RAN or in binary combinations of each one with RAN, RAN's RR of death was partially confounded by these other proteins (Fig. 5, Table 2). These results suggest that all 4 proteins lie on signalling pathways which increase the RR of patient death from metastatic disease. The partial nature of the confounding of RR for RAN by these other proteins suggests that other pathways not involving RAN are also involved in causing patient death. That the decline in RR for RAN with either Met or MMP2 at nearly 50 % (49 % or 48 %, respectively) was larger than the decline in RR for Met or MMP2 in binary combinations with RAN at nearly 1/3 (32 % for both) (Table 2) suggests that Met and MMP2 are more proximal members than RAN in the pathway leading to patient death. This suggestion is further supported by results in Fig. 5. Thus when staining data for MMP2 is added to that for RAN in the primary tumours, there is a significant decrease, but when staining data for RAN is added to that for MMP2, there is no significant decrease

in patient survival times. Practically when staining data for MMP2 is included with that for RAN, the RR for patient death is increased from the original 14.9 to 82.1 fold. This result is complemented when viewed the other way round with an enhanced NPR for both proteins of nearly 98 % compared to that for either protein alone (Table 3). Thus the in vivo studies support the in vitro studies that RAN and MMP2 can be used together to stratify prognosis of operable breast cancer patients and that this relationship is independent of another biomarker ERα present in the primary tumours (Supplementary Fig. S1).

5. Conclusion

In conclusion, we have established in cell line models of breast cancer a relationship between RAN and MMP2 and properties related to metastasis. The inclusion of MMP2 as well as RAN facilitates a more accurate prognosis and further identifies a subgroup of patients that could benefit more from conventional chemotherapy and from therapy directed against both proteins than against either one alone.

CRediT authorship contribution statement

Mohamed El-Tanani: Concept development, Experimental design and imaging, data analysis.

Yin-Fai Lee: Experimental work and imaging, data analysis.

Arwa Omar Al Khatib: Experimental work and imaging, data analysis.

Yusuf Haggag: Experimental work and imaging, data analysis.

Mark Sutherland: Experimental work and imaging, data analysis.

Shu-Dong Zhang: Experimental work and imaging, statical analysis.

Alaa A.A. Aljabali: Experimental work and imaging, data analysis.

Vijay Mishra: Experimental work and imaging, data analysis.

Ángel Serrano-Aroca: Experimental work and imaging, data analysis.

Murtaza M Tambuwala: Experimental work and imaging, data analysis.

Angela Platt-Higgins and Philip S Rudland: Provided resources and secured funding, experimental design.

All authors contributed towards the drafting of the initial draft and reading and approving final version for submission.

Ethics approval and consent to participate

Human materials and data were collected in an anonymised fashion under the legally-binding, UK Human Tissue Act supervised by the UK's National Research Ethical Committee (NREC) and approved by North West REC (Ref [12]/NW/0778), protocol number UOL000889, IRAS number 107845 to Prof. P.S. Rudland.

Consent for publication

All authors consent for publication.

Funding

Funded by Al-Ahliyya Amman University, Grow MedTech and Cancer and Polio Research Fund Ltd., UK (M. El-T, A.P-H, P.S.R).

Declaration of competing interest

The authors declare that they have no known competing financial interests or personal relationships that could have appeared to influence the work reported in this paper.

Data availability

Data will be made available on request.

Appendix A. Supplementary data

Supplementary data to this article can be found online at https://doi.org/10.1016/j.lfs.2022.121046.

References

[1] R.L. Siegel, K.D. Miller, H.E. Fuchs, A. Jemal, Cancer statistics, 2021, CA Cancer J. Clin. 71 (2021) 7–33.
[2] H.F. Yuen, K.K. Chan, C. Grills, et al., Ran is a potential therapeutic target for cancer cells with molecular changes associated with activation of the PI3K/Akt/mTORC1 and Ras/MEK/ERK pathways, Clin. Cancer Res. 18 (2012) 380–391.
[3] H.F. Yuen, V.K. Gunasekharan, K.K. Chan, et al., RanGTPase: a candidate for myc-mediated cancer progression, J. Natl. Cancer Inst. 105 (2013) 475–488.
[4] P.R. Clarke, C. Zhang, Spatial and temporal coordination of mitosis by ran GTPase, Nat. Rev. Mol. Cell Biol. 9 (2008) 464–477.
[5] K.B. Matchett, S. McFarlane, S.E. Hamilton, et al., Ran GTPase in nuclear envelope formation and cancer metastasis, Adv. Exp. Med. Biol. 773 (2014) 323–351.
[6] J.D. Moore, The ran-GTPase and cell-cycle control 23 (2001) 77–85.
[7] V.V. Kurisetty, P.G. Johnston, N. Johnston, et al., RAN GTPase is an effector of the invasive/metastatic phenotype induced by osteopontin, Oncogene 27 (2008) 7139–7149.
[8] F. Xia, C.W. Lee, D.C. Altieri, Tumor cell dependence on ran-GTP-directed mitosis, Cancer Res. 68 (2008) 1826–1833.
[9] R.P. Verma, C. Hansch, Matrix metalloproteinases (MMPs): chemical-biological functions and (Q)SARs, Bioorg. Med. Chem. 15 (2007) 2223–2268.
[10] B.P. Chen, G. Liang, J. Whelan, T. Hai, ATF3 and ATF3 delta zip. Transcriptional repression versus activation by alternatively spliced isoforms, J. Biol. Chem. 269 (1994) 15819–15826.
[11] T. Hai, T. Curran, Cross-family dimerization of transcription factors Fos/Jun and ATF/CREB alters DNA binding specificity, Proc. Natl. Acad. Sci. U. S. A. 88 (1991) 3720–3724.
[12] M. Janz, M. Hummel, M. Truss, et al., Classical hodgkin lymphoma is characterized by high constitutive expression of activating transcription factor 3 (ATF3), which promotes viability of Hodgkin/Reed-Sternberg cells, Blood 107 (2006) 2536–2539.
[13] B. Ma, A. Khazali, A. Wells, CXCR3 in carcinoma progression, Histol. Histopathol. 30 (2015) 781–792.
[14] S. Ma, C. Pang, L. Song, F. Guo, H. Sun, Activating transcription factor 3 is overexpressed in human glioma and its knockdown in glioblastoma cells causes growth inhibition both in vitro and in vivo, Int. J. Mol. Med. 35 (2015) 1561–1573.
[15] A.E. Pelzer, J. Bektic, P. Haag, et al., The expression of transcription factor activating transcription factor 3 in the human prostate and its regulation by androgen in prostate cancer, J. Urol. 175 (2006) 1517–1522.
[16] C.D. Wolfgang, B.P. Chen, J.L. Martindale, N.J. Holbrook, T. Hai, gadd153/Chop10, a potential target gene of the transcriptional repressor ATF3, Mol. Cell. Biol. 17 (1997) 6700–6707.
[17] N. Reynders, D. Abboud, A. Baragli, et al., The distinct roles of CXCR3 variants and their ligands in the tumor microenvironment, Cells 8 (2019).
[18] S.Y. Shin, J.S. Nam, Y. Lim, Y.H. Lee, TNFalpha-exposed bone marrow-derived mesenchymal stem cells promote locomotion of MDA-MB-231 breast cancer cells through transcriptional activation of CXCR3 ligand chemokines, J. Biol. Chem. 285 (2010) 30731–30740.
[19] H.F. Yuen, K.K. Chan, A. Platt-Higgins, et al., Ran GTPase promotes cancer progression via met receptormediated downstream signaling, Oncotarget 7 (2016) 75854–75864.
[20] C. Singh, S. Roy-Chowdhuri, Quantitative real-time PCR: recent advances, Methods Mol. Biol. 1392 (2016) 161–176.
[21] H.F. Yuen, C.M. McCrudden, K.K. Chan, et al., The role of Pea3 group transcription factors in esophageal squamous cell carcinoma, Am. J. Pathol. 179 (2011) 992–1003.
[22] E.H. Dakir, A. Pickard, K. Srivastava, et al., The anti-psychotic drug pimozide is a novel chemotherapeutic for breast cancer, Oncotarget 9 (2018) 34889–34910.
[23] H.F. Yuen, K.K. Chan, A. Platt-Higgins, et al., Ran GTPase promotes cancer progression via met recepto-rmediated downstream signaling, Oncotarget 7 (2016) 75854–75864.
[24] H.F. Yuen, Y.T. Chiu, K.K. Chan, et al., Prostate cancer cells modulate osteoblast mineralisation and osteoclast differentiation through Id-1, Br. J. Cancer 102 (2010) 332–341.
[25] H.F. Yuen, S.D. Zhang, A.S. Wong, et al., Regarding "Co-expression of SNAIL and TWIST determines prognosis in estrogen receptor-positive early breast cancer patients", Breast Cancer Res. Treat. 131 (2012) 351–352.
[26] P.S. Rudland, A. Platt-Higgins, C. Renshaw, et al., Prognostic significance of the metastasis-inducing protein S100A4 (p9Ka) in human breast cancer, Cancer Res. 60 (2000) 1595–1603.
[27] T.M. Ismail, D. Bennett, A.M. Platt-Higgins, M. Al-Medhity, R. Barraclough, P. S. Rudland, S100A4 elevation empowers expression of metastasis effector molecules in human breast cancer, Cancer Res. 77 (2017) 780–789.
[28] J.J. Xie, Y.M. Xie, B. Chen, et al., ATF3 functions as a novel tumor suppressor with prognostic significance in esophageal squamous cell carcinoma, Oncotarget 5 (2014) 8569–8582.
[29] H. Zhou, J. Wu, T. Wang, X. Zhang, D. Liu, CXCL10/CXCR3 axis promotes the invasion of gastric cancer via PI3K/AKT pathway-dependent MMPs production, Biomed. Pharmacother. 82 (2016) 479–488.

[30] H.B.P. Normand Pouliot, Allan Burrows, Investigating Metastasis Using In Vitro Platforms. Madame Curie Bioscience Database [Internet], Landes Bioscience, Austin (TX), 2013.
[31] G.P. Gupta, J. Massague, Cancer metastasis: building a framework, Cell 127 (2006) 679–695.
[32] P.S. Rudland, A. Platt-Higgins, M. El-Tanani, et al., Prognostic significance of the metastasis-associated protein osteopontin in human breast cancer, Cancer Res. 62 (2002) 3417–3427.
[33] Y. Liu, H. Ma, J. Yao, ERalpha, a key target for cancer therapy: a review, Onco. Targets. Ther. 13 (2020) 2183–2191.
[34] E.I. Deryugina, J.P. Quigley, Matrix metalloproteiases and tumor metastasis, Cancer Metastasis Rev. 25 (2006) 9–34.
[35] A. Kohrmann, U. Kammerer, M. Kapp, J. Dieti, J. Anacker, Expression of matrix metalloproteinases (MMPs) in primary human breast cancer and breast cancer cell lines: new findings and review of the literature, BMC Cancer 9 (2009) 188.
[36] A. Rizwan, M. Cheng, Z.M. Bhujwalla, B. Krishnamachary, L. Jiang, K. Glunde, Breast cancer cell adhesion and degradome interact to drive metastasis, npj Breast Cancer 1 (2015) 15017.
[37] T. Okegawa, R.C. Pong, J.T. Hsieh, The role of cell adhesion molecule in cancer progression and its application to cancer therapy, Acta Biochim. Pol. 51 (2004) 445–457.
[38] Y. Jiao, X. Feng, Y. Zhan, R. Wang, S. Zheng, W. Liu, et al., Matrix metalloproteinase-2 promotes alphavbeta3 integrin-mediated adhesion and migration of human melanoma cells by cleaving fibronectin, PLoS One 7 (2012), e41591.
[39] H.A. Kenny, E. Lengyel, MMP-2 functions as an early response protein in ovarian cancer metastasis, Cell Cycle 8 (2009) 683–688.
[40] H.A. Kenny, S. Kaur, L.M. Coussens, E. Lengyel, The initial steps of ovarian cancer cell metastasis are mediated by MMP-2 cleavage of vitronectin and fibronectin, J. Clin. Invest. 118 (2008) 1367–1379.
[41] S. Li, W. Luo, Matrix metalloproteinase 2 contributes to aggressive phenotype, epithelial-mesenchyme transition and poor outcome in nasopharyngeal carcinoma, Onco. Targets. Ther. 12 (2019) 5701–5711.
[42] H. Wang, Y. Ou, J. Ou, Z. Jian, Fli1 promotes metastasis by regulating MMP2 signaling in hepatocellular carcinoma, Mol. Med. Rep. 17 (2018) 1986–1992.
[43] L. Koren, U. Barash, Y. Zohar, N. Karin, A. Aronheim, The cardiac maladaptive ATF3-dependent cross-talk between cardiomyocytes and macrophages is mediated by the IFNgamma-CXCL10-CXCR3 axis, Int. J. Cardiol. 228 (2017) 394–400.